HHS Public Access

Author manuscript

Hum Genet. Author manuscript; available in PMC 2022 June 30.

Published in final edited form as:

Hum Genet. 2021 July ; 140(7): 1061–1076. doi:10.1007/s00439-021-02274-3.

Pathogenic variants in *CDH11* impair cell adhesion and cause Teebi hypertelorism syndrome

Dong Li[1], **Michael E. March**[1], **Paola Fortugno**[2,3], **Liza L. Cox**[4], **Leticia S. Matsuoka**[1], **Rosanna Monetta**[2,3], **Christoph Seiler**[5], **Louise C. Pyle**[6], **Emma C. Bedoukian**[6], **María José Sánchez-Soler**[7], **Oana Caluseriu**[8,9], **Katheryn Grand**[10], **Allison Tam**[11], **Alicia R. P. Aycinena**[11], **Letizia Camerota**[3], **Yiran Guo**[1], **Patrick Sleiman**[1,12], **Bert Callewaert**[13,14], **Candy Kumps**[13], **Annelies Dheedene**[13], **Michael Buckley**[15], **Edwin P. Kirk**[15,16], **Anne Turner**[16], **Benjamin Kamien**[17], **Chirag Patel**[18], **Meredith Wilson**[19], **Tony Roscioli**[15,16,20], **John Christodoulou**[21,22,23], **Timothy C. Cox**[4], **Elaine H. Zackai**[12,24], **Francesco Brancati**[3,25,26], **Hakon Hakonarson**[1,12,24], **Elizabeth J. Bhoj**[1,12,24]

[1]Center for Applied Genomics, The Children's Hospital of Philadelphia, Philadelphia, PA, USA

[2]Laboratory of Molecular and Cell Biology, Istituto Dermopatico dell'Immacolata, IDI-IRCCS, Rome, Italy

[3]Department of Life, Health and Environmental Sciences, University of L'Aquila, L'Aquila, Italy

[4]Departments of Oral and Craniofacial Sciences and Pediatrics, University of Missouri-Kansas City School of Dentistry, Kansas City, MO 64108, USA

[5]Zebrafish Core Facility, The Children's Hospital of Philadelphia Research Institute, Philadelphia, PA, USA

[6]Individualized Medical Genetics Center, Division of Human Genetics, The Children's Hospital of Philadelphia, Philadelphia, PA, USA

[7]Sección de Genética Médica, Servicio de Pediatría, Hospital Clínico Universitario Virgen de la Arrixaca, IMIB-Arrixaca, Murcia, España

[8]Department of Medical Genetics, University of Alberta, Edmonton, AB T6G 2H7, Canada

[9]The Stollery Pediatric Hospital, Edmonton, AB T6G 2H7, Canada

[10]Department of Pediatrics, Cedars-Sinai Medical Center, Los Angeles, CA, USA

✉Dong Li lid2@email.chop.edu, Elizabeth J. Bhoj bhoje@email.chop.edu.

Dong Li and Michael E. March contributed equally to this work.

Author contribution DL, MB, EPK, TCC, and HH contributed to the molecular evaluation of the affected individuals. LCP, ECB, MSS, OC, KG, AT, APA, LC, BC, CK, AT, BK, CP, MW, TR, EHZ, and EJB contributed to the clinical evaluation of the affected individuals. DL, MEM, PF, LLC, LSM, RM, CS, and FR contributed to the functional investigations. YG, PS, AD, and JC coordinated to the research study subject enrollment. All the authors read, edited, and approved the manuscript.

Declarations

Conflict of interest None of the authors has any conflicts of interests to declare.

Supplementary Information The online version contains supplementary material available at https://doi.org/10.1007/s00439-021-02274-3.

Consent to participate and publish All the patients' families from the different institutions agreed to participate and publish in this study and signed appropriate consent forms. The Institutional Review Board of The Children's Hospital of Philadelphia approved this study. We obtained photo consent for including patients' photographs from The Children's Hospital of Philadelphia, Hospital Clínico Universitario Virgen de la Arrixaca, Ghent University Hospital, and Sydney Children's Hospital.

[11]Division of Medical Genetics, Department of Pediatrics, University of California, San Francisco, San Francisco, CA, USA

[12]Department of Pediatrics, Perelman School of Medicine, University of Pennsylvania, Philadelphia, PA, USA

[13]Center for Medical Genetics, Ghent University Hospital, Ghent, Belgium

[14]Department of Biomolecular Medicine, Ghent University, Ghent, Belgium

[15]NSW Health Pathology Genomics Laboratory, Prince of Wales Hospital, Randwick, NSW, Australia

[16]Centre for Clinical Genetics, Sydney Children's Hospital, Randwick, NSW, Australia

[17]Genetic Services of Western Australia, King Edward Memorial Hospital, Perth, Australia

[18]Genetic Health Queensland, Royal Brisbane and Women's Hospital, Brisbane, QLD, Australia

[19]Department of Clinical Genetics, Children's Hospital at Westmead, Sydney, NSW, Australia

[20]Neuroscience Research Australia and Prince of Wales Clinical School, University of New South Wales, Kensington, NSW, Australia

[21]Murdoch Children's Research Institute, Melbourne, Australia

[22]Department of Paediatrics, University of Melbourne, Melbourne, Australia

[23]Discipline of Child and Adolescent Health, Sydney Medical School, University of Sydney, Sydney, Australia

[24]Division of Human Genetics, The Children's Hospital of Philadelphia, Philadelphia, PA, USA

[25]Institute of Translational Pharmacology, National Research Council, Rome, Italy

[26]IRCCS San Raffaele Pisana, Rome, Italy

Abstract

Teebi hypertelorism syndrome (THS; OMIM 145420) is a rare craniofacial disorder characterized by hypertelorism, prominent forehead, short nose with broad or depressed nasal root. Some cases of THS have been attributed to *SPECC1L* variants. Homozygous variants in *CDH11* truncating the transmembrane and intracellular domains have been implicated in Elsahy–Waters syndrome (EWS; OMIM 211380) with hypertelorism. We report THS due to *CDH11* heterozygous missense variants on 19 subjects from 9 families. All affected residues in the extracellular region of Cadherin-11 (CHD11) are highly conserved across vertebrate species and classical cadherins. Six of the variants that cluster around the EC2–EC3 and EC3–EC4 linker regions are predicted to affect Ca^{2+} binding that is required for cadherin stability. Two of the additional variants [c.164G > C, p.(Trp55Ser) and c.418G > A, p.(Glu140Lys)] are also notable as they are predicted to directly affect *trans*-homodimer formation. Immunohistochemical study demonstrates that CDH11 is strongly expressed in human facial mesenchyme. Using multiple functional assays, we show that five variants from the EC1, EC2–EC3 linker, and EC3 regions significantly reduced the cell-substrate *trans* adhesion activity and one variant from EC3–EC4 linker results in changes in cell morphology, focal adhesion, and migration, suggesting dominant negative effect. Characteristic

features in this cohort included depressed nasal root, cardiac and umbilical defects. These features distinguished this phenotype from that seen in *SPECC1L*-related hypertelorism syndrome and *CDH11*-related EWS. Our results demonstrate heterozygous variants in *CDH11*, which decrease cell–cell adhesion and increase cell migratory behavior, cause a form of THS, as termed *CDH11*-related THS.

Introduction

The *CDH11* gene encodes Cadherin-11, a member of the superfamily of cadherins, which are key molecules implicated in cell–cell adhesion and play critical roles in embryonic morphogenesis with tightly regulated spatial and temporal expression in species ranging from *C. elegans* and *Drosophila* to mouse and human (Nishimura and Takeichi 2009; Borchers et al. 2001; Hyafil et al. 1981; Cavey et al. 2008; Takeichi 1995; Tepass 1999). Cadherins are categorized into four subfamilies based on their domain layout and number of extracellular cadherin (EC) domain repeats: classical cadherins (type I and II), desmosomal cadherins, protocadherins, and atypical cadherins (including FAT, Dachsous, and Flamingo/CELSR) (Brasch et al. 2012; Yagi and Takeichi 2000). Classical cadherins that share a conserved cytoplasmic domain and an extracellular region consisting of five tandem EC repeats (EC 1–5) represent the most characterized subfamily. Type 1 cadherins are encoded by the human *CDH1*, *CDH2*, *CDH3*, and *CDH4* genes. Type II, defined by the absence of the histidine–alanine–valine (HAV) motif from the EC1 repeat, are encoded by human *CDH5*, *CDH7*, *CDH8*, *CDH11*, and *CDH12* genes (Takeichi 1995; Tepass et al. 2000). Cadherin-11, also known as osteoblast (OB)-cadherin as it was identified initially in a mouse osteoblastic cell line and human osteosarcoma (Okazaki et al. 1994), is a member of transmembrane adhesive receptors, and consists of 796 amino acids. It is divided structurally into a signal peptide, a cadherin propeptide, 5 EC domain repeats of approximately 110 amino acids each (EC 1–5), a transmembrane domain, and a conserved cytoplasmic domain which links catenins to the actin and microtubule cytoskeleton (Okazaki et al. 1994).
It is believed that Cadherin-11 forms two types of dimers. Lateral association between Cadherin-11 monomers, dependent on the binding of extracellular Ca^{2+} in the linker domains between each EC domain, forms a *cis* dimer within the same plasma membrane, while in adherens junctions, Cadherin-11 protrudes to form a *trans* dimer (via its first EC domain repeat) from an opposing cell surface (Patel et al. 2006). Cytoplasmic interactions with Cadherin complexes stabilize cell–cell junctions by reorganizing the actin cytoskeleton. Thus, Cadherin-11 is involved in dynamic control of cell–cell adhesion activity, and in turn, can regulate cell migration and cell signaling during a variety of developmental processes (Borchers et al. 2001).

Teebi hypertelorism syndrome (THS; OMIM 145420) was first described in a large four-generation family, in which dysmorphic features including hypertelorism, proptosis and ptosis segregated as an autosomal dominant trait (Teebi 1987). This craniofacial condition was subsequently reported by multiple authors in 16 additional families (Bhoj et al. 2015; Hoffman et al. 2007; Koenig 2003; Machado-Paula and Guion-Almeida 2003; Nakagawa et al. 1998; Stratton 1991; Toriello and Delp 1994; Tsai et al. 2002; Tsukahara et al. 1995; Bhoj et al. 2019; Zhang et al. 2020; Han et al. 2006). We and others recently reported rare

missense variants in *SPECC1L*, a gene encoding a cytoskeletal protein involved in cell–cell adhesion and migration, in five families with a clinical diagnosis of THS (Bhoj et al. 2015, 2019; Zhang et al. 2020).

Like many other rare diseases, the genetic etiology of these individuals remains unknown for at least half of the patients, with the underlying molecular and cellular mechanisms undetermined. As an expansion of our study focused on the identification of genetic causes of rare craniofacial disorders, here we report 19 individuals with heterozygous variants in *CDH11* and THS assembled through international collaborations. We identified nine different missense variants in the extracellular domain that are predicted to affect homodimer formation in 3D structure. Cell-to-substrate adhesion study confirmed that all of the five studied variants reduced the adhesion function, which was in accordance with our structural modeling predictions. Moreover, we obtained fibroblasts from one individual and morphology study demonstrated that CHD11 is involved in focal adhesion and actin cytoskeleton organization. Consistent with decreased cell–cell adhesion activity, affected individual's fibroblasts demonstrated accelerated cell migration activity. Together, these data describe THS can be caused by pathogenic heterozygous missense in *CDH11*, as termed *CDH11*-related THS by following the dyadic approach to delineate Mendelian genetic disorders (Biesecker et al. 2021).

Materials and methods

Research participants and genetic analysis

Informed consent was obtained from all the families according to protocols approved by local institutional review boards and human research ethics committees. Permission for clinical photographs was given separately. Genomic DNA was extracted from whole blood from the affected children and their unaffected family members. Exome sequencing was performed with a variety of standard capture kits and data analysis was performed independently. For kindreds A–F, research exome sequencing and genetic analysis was performed using the Agilent V5 and Illumina HiSeq2500 at Center for Applied Genomics at The Children's Hospital of Philadelphia. Data were quality controlled and analyzed using a custom-built pipeline that incorporates BWA-mem v0.7.12 for alignment, Picard v1.97 for PCR duplication removal, and GATK v2.6.5 for variant calling. ANNOVAR and SnpEff were used to functionally annotate the variants and collect minor allele frequency data from 1000 Genomes Projects, ESP6500SI, ExAC, gnomAD, and Kaviar. Relatively common variants for suspected autosomal dominant mode of inheritance were excluded based on MAF threshold of 0.1% in either population dataset, and functional annotation, such as synonymous, non-exonic, and non-splicing-altering. Subsequent gene prioritization was performed on the basis of deleterious prediction and biological relevance by referring to the Online Mendelian Inheritance in Man (OMIM) database and Human Gene Mutation Database (HGMD). Similarly, research exome was performed on five affected family members of kindred H. For kindred G and I, clinical exome was performed using the MedExome SeqCap EZ assay (Roche-Nimblegen, CA) and SureSelectXT Low Input Human All Exon v7 (Agilent Technologies), respectively; and sequenced with Illumina NextSeq 500 (Illumina, CA) and Illumina NovaSeq 6000, respectively. Validation of *CDH11*

candidate variants in all of the available affected or unaffected family members of all the families was performed by standard Sanger sequencing.

Immunohistochemical analysis of human embryonic facial tissue

Immunohistochemical study was performed on coronal sections of human embryonic facial tissues from 67 to 72 days gestation. Human fetal tissues were recovered, with consent, at the Human Birth Defects Research Laboratory, University of Washington. The age of specimens was estimated as previously described (Cox et al. 2018). Embryonic facial tissue was embedded in paraffin and sectioned at 4-micron thickness in the coronal plane. Sections were then stained with a primary antibody against human CDH11 (SantaCruz #sc-365867 [F-3]) followed by a Goat anti-mouse (Millipore-Sigma; DC02L) HRP-conjugated secondary antibody.

L cell transductions

L cells were acquired from ATCC. CDH11-WT and mutant sequences were cloned into the pBabe-Puro-CMV + vector via the HiFi cloning system (NEB) and verified by Sanger sequencing. Retroviral transductions were performed by cotransfection of CDH11 expression plasmids with packaging and envelope plasmids into 293Ts using FugeneHD (Promega). Viral supernatants were supplemented with 8 μg/ml polybrene, filtered through 0.45-micron filters, and applied to L cells. L cells were transduced by spinfection at 650×g for 90 min, cultured for 2 days, and selected with 1 μg/ml puromycin. Resistant cells were enriched for expression with two rounds of bead selection, using anti-CDH11 antibody (R&D Systems, MAB17901) and Dynabeads Goat anti-mouse IgG (Invitrogen) using the manufacturer's protocol for "Direct Technique" isolation. The same antibody was used in conjunction with a PE-labeled goat anti-mouse secondary antibody to monitor expression by flow cytometry.

Adhesion assay

The protocol for the adhesion assay will refer to the following solutions: Culture medium —Dulbecco's modified essential medium (ThermoFisher #10569–010) + 10% fetal bovine serum; HBSS/Ca—Hank's buffered salt solution containing 1 mM $CaCl_2$ and no magnesium (ThermoFisher #14170–112 supplemented with 1 mM $CaCl_2$); Binding buffer—20 mM HEPES, 150 mM NaCl, 1 mM $CaCl_2$, 3 mM KCl, pH 7.4; TBS/Ca—50 mM Tris pH 7.5, 150 mM NaCl, 1 mM $CaCl_2$. 96-well microtiter plates (Immulon 4HBX plates, Thermo-Scientific #3855) were coated with indicated amounts of recombinant CDH11-Fc fusion protein (R&D Systems) in TBS/Ca in 50 μl total volume, overnight at 4 °C. Wells with no protein were incubated with TBS/Ca alone. Wells were washed twice with 200 μl binding buffer, and blocked with 100-μl binding buffer containing 1% bovine serum albumin for 2 h at room temperature. Wells were washed twice with binding buffer, and once with binding buffer containing 1% fetal bovine serum. During the blocking of the plate, cells were harvested and labeled. L cells in 10-cm dishes were harvested by washing once with 10 ml HBSS/Ca, and trypsinizing with 2 ml 0.05% trypsin (ThermoFisher #15090–046) in HBSS/Ca. Trypsin was neutralized with 8-ml culture medium. 3 million cells were pelleted and washed with 10 ml HBSS/Ca, and resuspended in 1 ml HBSS/Ca containing 2 μM Calcein-AM (ThermoFisher #C3100MP). Cells were incubated at 37 °C for 15 min, 5 ml of

culture medium was added, and cells were incubated at 37 °C for a further 5 min. Labeled cells were washed once with binding buffer, resuspended in 1 ml binding buffer containing 1% fetal bovine serum, and counted. Volumes were adjusted so the final cell concentrations were 1 million cells/ml. 100 μl of cell suspension (100,000 cells) was added to wells of the coated microtiter plate. The plate was centrifuged at 20×*g* for 2 min, and placed at 37 °C for 3 h. After incubation, the plate was read on a fluorescent plate reader (SpectraMax i3, Molecular Devices) with excitation at 485 nm and emission at 535 nm. The results of this first read were used as the input. The plate was washed with binding buffer six times, and read again. The second read results were used as the bound value. Both input and bound values were adjusted by subtracting the background fluorescence of the plate, obtained as the average of the values of all the empty wells on the plate. Percent bound numbers were generated for each well by dividing the background-adjusted bound values by the background-adjusted input values.

Results

Identification of heterozygous variants in *CDH11* in THS

As an expansion of our study focused on the identification of genetic causes of rare craniofacial disorders, we performed exome sequencing of nine additional participants and their available parents from six families with either suspected de novo THS or autosomal dominant transmission of clinical features resembling THS. We identified six novel heterozygous missense variants in the *CDH11* gene in nine individuals from six independent families [c.164G > C, p.(Trp55Ser); c.418G > A, p.(Glu140Lys); c.778G > A, p.(Asp260Asn); c.780 T > A, p.(Asp260Glu); c.785A > T, p.(Asn262Ile); and c.979G > T, p.(Gly327Trp)] (Table S1; Fig. 1a). Of these six missense variants, which were not found in population genomics resources (i.e., 1000 Genomes Project, ESP6500SI, and gnomAD) and were predicted to be deleterious by multiple prediction algorithms (SIFT, Polyphen2, LRT, MutationTaster, CADD, etc.) (Table S1), three were confirmed to have occurred de novo, two were dominantly inherited in two families with seven affected individuals, and one was identified in an adopted singleton. Independently, three more families with *CDH11* heterozygous variants [c.835G > C, p.(Glu279Gln); c.1121 T > A, p.(Val374Glu); and c.797C > T, p.(Pro266Leu)], two of which are absent in the population databases as well (Table S1), were identified by exome sequencing and recruited through personal collaborations and GeneMatcher (Sobreira et al. 2015) (Fig. 1a; Tables S1, S2). Variants p.(Glu279Gln) and p.(Pro266Leu), were then confirmed de novo and the variant p.(Val374Glu) was shared among all six affected members of a family from Australia.

Clinical summary

All the patients had typical craniofacial features of THS as summarized in Table 1 evaluated independently by the primary clinicians, and detailed data can be found in Table S2 (see also Fig. 2). The defining feature of ocular hypertelorism was seen in all individuals (100%), with a broad or high forehead in 18 of 19 individuals (95%; 10 individuals with large anterior fontanelle), thick and/or broad eyebrows in 17 of 19 individuals (89%), a depressed nasal root in 13 of 19 individuals (68%), a broad nasal tip in 18 of 19 individuals (95%), and a short nose in 15 individuals (79%). Similarly, a thin upper lip (84%), a small chin with

horizontal crease (84%), and a high palate or cleft palate (68%) were frequently observed, whereas a few facial dysmorphic features were less frequently seen, including proptosis (26%), ptosis (26%), an everted lower lip (37%), small teeth (16%), and delayed tooth eruption (16%). Of interest, 2 of 19 individuals (11%) were noted to have a subtle coloboma of the upper eyelid (Individuals four and seven), which has not been previously reported as a feature of THS. Occasional abnormalities of the extremities, including tapered fingers, short distal phalanges, broad thumb/big toes, small hands/feet, long/short toes, bulbous tips of toes, broad feet, and clinodactyly of the fifth fingers/toes, were seen in 9 of 18 individuals (50%). Developmental delay and intellectual disability were variable in seven individuals (37%) ranging from very mild speech delay in five individuals to global delay in individual 10. Behavioral issues, i.e., autism and attention-deficit hyperactivity disorder (ADHD) were formal diagnosed only in kindred F (individuals 8 and 10). 12 of 19 individuals (63%) had normal overall development.

Molecular and structural analyses of *CDH11* variants

Remarkably, all of the nine missense variants that we identified [p.(Trp55Ser), p.(Glu140Lys), p.(Asp260Asn), p.(Asp260Glu), p.(Asn262Ile), p.(Pro266Leu), p.(Glu279Gln), p.(Gly327Trp), and p.(Val374Glu)] affect residues of the extracellular cadherin repeats, each of which has been shown to be highly conserved among vertebrate orthologs and may contribute to the formation of *cis* and *trans* dimers (Zhu et al. 2003; Chappuis-Flament et al. 2001) (Fig. 1b). In addition, we noted that six out of nine variants [p.(Asp260Asn), p.(Asp260Glu), p.(Asn262Ile), p.(Pro266Leu), p.(Glu279Gln), and p.(Val374Glu)] are very close to the EC1–EC2 and EC2–EC3 linker regions, and one [p.(Trp55Ser)] involves the highly conserved tryptophan anchor residue (referred to as W2 after signal peptide and propeptide cleavage) that is critical for *trans* dimer formation in the homologous CDH family members (Kitagawa et al. 2000; Tamura et al. 1998) (Fig. 1b).

An intolerance landscape plot was generated by the MetaDome server (Wiel et al. 2019). It indicated that EC1, EC2, and the EC1–EC2 and EC2–EC3 linker regions were the most intolerant regions for the missense variants, where the variants p.(Glu140Lys), p.(Asp260Glu), p.(Asp260Asn), p.(Asn262Ile), and p.(Pro266Leu), affecting residues with the lowest d_N/d_S scores (indicating more intolerance to a missense change), are located (Fig. 1c; Table S1). On the other hand, variants p.(Gly327Trp), p.(Trp55Ser), p.(Glu279Gln), and p.(Val374Glu) were less intolerant, with slightly higher scores (Fig. 1c; Table S1). Moreover, all of the eight affected residues are highly conserved across vertebrate species, as well as within four additional classical type I and II cadherins (Fig. 1d). Collectively, these provide supportive evidence for pathogenicity of the missense variants identified. We further mapped the variants identified in *CDH11* onto *CDH1*, a paralogous gene of *CDH11* and implicated in a number of autosomal dominant human disorders (MIM: 137215 and 119580) (Cox et al. 2018; Ghoumid et al. 2017; Kievit et al. 2018; Brito et al. 2015; Guilford et al. 1998; Richards et al. 1999), and found that all but one of their corresponding paralogous residue changes (p.Pro373Leu) in *CDH1* were also absent from gnomAD (Table S1), lending a further support of the intolerant nature of the variants that we identified in *CDH11*. Even so, the *CDH1* variant Pro373Leu was identified in hereditary diffuse gastric cancer and has been shown to be pathogenic through human cell in vitro assays and a zebrafish model (Kievit et

al. 2018; Corso et al. 2007), suggesting its paralogous gene *CDH11* variant p.(Pro266Leu) could be pathogenic.

To further explore the structural impact of the nine missense variants, the three-dimensional structures of the EC domains of wild-type and mutant CDH11 (amino acids 54–375) were obtained using homology modeling with SWISS-MODEL and displayed with Chimera UCSF (Guex and Peitsch 1997; Pettersen et al. 2004). First, the crystallographic structure of homodimeric EC1–EC2 domains of mouse cadherin-11 at a 3.2 Å resolution was used as a template as it exhibits 99.52% identity with human CDH11 (PDB: 2a4e) (Patel et al. 2006). As shown in Fig. 3a, residue Trp55 forms hydrogen bonds with both Glu140 and Pro141 from the partner chain (Fig. 3b). Replacement of Trp55 with serine, the side chain changing from a large aromatic residue to a small neutral one, was predicted to result in loss of a hydrophobic interaction with Pro141 from the partner chain (Fig. 3c). Replacement of Glu140 with lysine, a negatively charged to a positively charged side chain, was also predicted to disrupt the hydrophobic interaction with Trp55 from the partner chain (Fig. 3d). A previous study of N-cadherin has shown that the hydrogen bond involving the paralogous tryptophan residue is necessary for dimer formation and facilitates a subsequent conformational change that allows Ca^{2+} binding and stabilization of the *trans* dimer (Vunnam and Pedigo 2011). Together, these findings suggest that both p.(Trp55Ser) and p.(Glu140Lys) may modify the Ca^{2+}-binding pocket, and therefore, potentially affect the adhesive function.

Since residues Asp260 and Asn262, which lie in EC2–EC3 linker region, are not modeled in the available mouse cadherin-11 structure (PDB: 2a4e), we next used the mouse cadherin-8 monomer (X-ray; 4.5 Å; PDB: 2a62) (Patel et al. 2006) as a template to model the EC1–EC3 domains (amino acids 54–375). Both residues, lying in the Ca^{2+}-binding pocket between EC2 and EC3, form hydrogen bonds with multiple residues and provide a structural base for Ca^{2+} binding (Figs. S1A, S1B). Similarly, substitution of Asp260 with glutamic acid, a small to large side chain change, was predicted to abolish the hydrophobic interaction with Asn300 and lead to a more ‘open’ state of the Ca^{2+}-binding pocket (Fig. S1C). A similar finding was also observed when Asn262 is substituted by a large isoleucine (Fig. S1E). By contrast, the p.(Asp260Asn) change seems to keep the Ca^{2+}-binding pocket unaltered (Fig. S1D). Lastly, we pursued this further by mapping these missense variants onto a mouse E-cadherin protein structure (PDB: 3q2v) and demonstrated six missense variants [p.(Asp260Glu), p.(Asp260Asn), p.(Asn262Ile), p.(Pro266Leu), p.(Glu279Gln), and p.(Val374Glu)] cluster around the linker regions (Fig. S2), which suggests these six missense variants may change Ca^{2+} binding ability and in turn have an impact on protein adhesive function.

Functional studies of *CDH11* variants

We performed immunohistochemical study on coronal sections of human embryonic facial tissues from 67 to 72 days gestation. It showed strong staining of CDH11 in facial mesenchyme at the mid-palatal region (Fig. 4a) as well as at the level of the posterior palate (Fig. 4b), including the central palatal mesenchyme, dental mesenchyme, the eye and

optic muscles, and the tongue. This highlighted CDH11 protein is strongly expressed in the human developing face, in accordance with the human phenotype.

To functionally assess the missense variants identified in this study, we used L cells, a transformed mouse fibroblast line expressing no cadherins and widely used to study cell–cell adhesion in the cell-to-substrate adhesion assay (Okazaki et al. 1994; Kawaguchi et al. 1999; Accogli et al. 2019). Previous studies showed transient transfection of *CDH11* into L cells led to the acquisition of the ability to bind to cadherin-11 as either a purified protein or a surface-expressed protein on other cells (Okazaki et al. 1994; Kawaguchi et al. 1999). We transduced L cells using a retroviral vector for stable expression with one of the following constructs: CDH11-WT or the variants CDH11-Trp55Ser, CDH11-Glu140Lys, CDH11-Asp260Asn, CDH11-Asn262Ile, or CDH11-Gly327Trp. Similar levels of protein expression of wild type and the mutants were observed by flow cytometry (Fig. S3). L cells expressing CDH11-WT bound to hCadherin-11-Fc in a dose-dependent manner (Fig. 5a). However, binding of L cells transduced with three mutant constructs (CDH11-Trp55Ser, CDH11-Glu140Lys, and CDH11-Gly327Trp) constantly showed minimal binding (<< 1%) even when the hCadherin-11-Fc coated concentration increased, while two other mutants (CDH11-Asp260Asn and CDH11-Asn262Ile) demonstrated weaker binding compared to CDH11-WT. At the hCadherin-11-Fc amount of 187.5, 375, and 750 ng, the percentage of binding between WT and all of the five mutants differed significantly (Fig. 5a). These results indicate that the *CDH11* variants affect the cell–cell adhesion function, which was consistent with our structural modeling predictions.

To determine if the variant p.(Glu279Gln) impairs cell morphology, migration, and proliferation, we obtained fibroblasts from individual 12 (Kindred G), and compared to two control fibroblast lines from unrelated age-, gender-, and ethnicity-matched individuals. We confirmed expression of Cadherin-11 in control primary human dermal fibroblasts and determined its cellular distribution by immunostaining analysis. Cadherin-11 was expressed and localized in small spots at randomly distributed sites, particularly at the leading extending edge, along the protruding filopodial structures and at the cell–cell contact sites (Fig. S4A). An increased expression was observed in the affected individual's fibroblasts (Fig. S4A), which also was confirmed by Western blotting (Fig. S4B). Interestingly, whilst individual 12′s fibroblasts adhered to the substrate with an efficiency comparable to that observed in control cells (Fig. S4C) during the initial phases of adhesion (i.e., up to 2 h after plating), a strong alteration of cell morphology was observed (Fig. 5b). Control fibroblasts rapidly spread on plastic surface, however, individual 12′s fibroblasts remained smaller and rounder for a longer time, presenting delayed formation of lamellipodia and an abnormal membrane-protrusion dynamic with preferential formation of blebs and ruffles (Fig. 5b). A large number of focal adhesions were present in individual 12′s fibroblasts, both at the leading edge and in the center of the cell, as evidenced by paxillin staining (Fig. 5c). However, differently from control fibroblasts that presented the typical focal contact punctate stain inter-connected with the stress fiber tips at the leading edge of spreading cells, focal adhesion structures in the individual 12 were immature and actin stress fibers were absent (Fig. 5c). Interestingly, staining for Cadherin-11 showed protein aggregates colocalizing with actin bundles 2 h after plating (Fig. 5d). In parallel, we used the same fibroblasts from individual 12 to carry out in vitro wound healing assay by means of

a wound artificially generated in vitro in a confluent cell monolayer. In agreement with previous observations that Cadherin-11 mutants lacking the extracellular domain behaves as a hypermorph in regard to CNC cells migration (Borchers et al. 2001; Kashef et al. 2009), individual 12′s fibroblasts were able to colonize the cell-free zone approximately twofold faster than control cells (Fig. 5e). Finally, we observed no measurable differences in proliferation in three replicates between individual 12′s fibroblasts and control fibroblasts (Fig. S4D).

Discussion

In this study, we report on 19 subjects from 9 families harboring de novo or dominantly inherited heterozygous missense variants in the extracellular domain of CDH11. Functional studies evoke an involvement of Cadherin-11 in focal adhesion and actin cytoskeleton organization and that variants in the extracellular domain lead to a reduced *trans* adhesion, but accelerated migration. Previous data showed that Cadherin-11 mediates cell-substrate adhesion by physically interacting with focal adhesions (Langhe et al. 2016), and that the extracellular domain is dispensable for promoting cell-substrate adhesion, cell protrusive activity, and cell migration, but at a fast pace (Kashef et al. 2009; Langhe et al. 2016). In a *Xenopus* graft model, grafted cranial neural crest cells overexpressing wild-type *Xenopus* cadherin-11 lost the ability to migrate to the branchial arches (Borchers et al. 2001). By contrast, overexpressing a mutant that deleted 72 amino acids between EC1 and EC2 in grafts led to accelerated migration of cells to the branchial arches (Borchers et al. 2001). Both overexpression graft models resulted in altered expression of cranial neural crest markers, suggesting that, in *Xenopus*, the cadherin-11-mediated migration process of cranial neural crest cells must be tightly balanced. Interestingly, co-expression of wild type and this mutant partially inhibited and rescued the early migration, instead of blocking migration. This indeed suggests that the deletion mutant exhibited a dominant negative effect, rather than loss-of-function (LoF) (Borchers et al. 2001). Of note, homozygous truncating variants in *CDH11* were previously reported in four families with Elsahy–Waters syndrome (EWS) (MIM: 211380), following autosomal recessive mode of inheritance (Castori et al. 2018; Harms et al. 2018; Taskiran et al. 2017). Although limited functional studies were performed on these truncating variants in previous studies, it is likely that they exert a LoF effect. Our results suggest that the identified missense variants exert a dominant negative effect, though a loss-of-function mechanism is also possible. Interestingly, the study in *Xenopus* also identified the expression of a neural crest marker, *twist*, is strongly reduced when overexpressing the dominant negative variant (Borchers et al. 2001). Of note, pathogenic variants of its orthologue *TWIST1* in human have been implicated in Saethre–Chotzen syndrome with hypertelorism. We speculate that the missense variants in CDH11 reduced *trans* adhesion and increased cell migration may alter the critical gene expression in the early embryonic development and result in hypertelorism. Moreover, other cadherins have been implicated in autosomal dominant or recessive Mendelian disorders, including aforementioned heterozygous variants of *CDH1* (encoding epithelial cadherin) in blepharocheilodontic syndrome (MIM: 119580), isolated and familial non-syndromic cleft lip with or without cleft palate, as well as diffuse gastric cancer with or without cleft lip and/or palate (MIM: 137215); *CDH3* (i.e., placental cadherin) biallelic pathogenic variants

causative of ectodermal dysplasia, ectrodactyly, and macular dystrophy (MIM: 225280) (Kjaer et al. 2005), and congenital hypotrichosis with juvenile macular dystrophy (MIM: 601553) (Sprecher et al. 2001); and more recently pathogenic heterozygous variants of *CDH2* (i.e., neuronal cadherin) in a syndromic neurodevelopmental disorder (Accogli et al. 2019). The phenotypes appears to correlate with the tissue types where the cadherins are most predominantly expressed as how they were originally named.

It is noteworthy that the four families with the previously described homozygous *CDH11* variants (causing EWS) and the nine families we present here with heterozygous variants in *CDH11* share some general craniofacial features, including hypertelorism, proptosis, ptosis, a broad forehead, broad and thick eyebrows, a short nose with a broad nasal tip, and a thin upper lip. However, these two cohorts of individuals are vastly different in the prevalence and severity of developmental delay/intellectual disability and skeletal abnormalities, which is quantified in Table 1. There are clearly two distinct phenotypes, as even after these patients had a heterozygous *CDH11* variant identified, a diagnosis of EWS was not considered as the phenotype was too divergent.

The vast majority (18/19) individuals in this study had normal or only minor developmental delays. All the patients with EWS have global developmental delay. Only two subjects with heterozygous *CDH11* missense variants have truncal skeletal findings, specifically pectus excavatum and vertebral fusions. Conversely, cardiac and umbilical defects were only found in individuals with heterozygous *CDH11* missense variants and are not with any EWS patients. However, only five subjects with EWS have been reported so far, and it is possible that cardiac and umbilical phenotypes will be observed in future individuals with such variants. Small eyelid coloboma was highlighted in one of the five EWS subjects (Harms et al. 2018). Interestingly, two individuals in our cohort were also noted to have very small colobomas of the upper eyelid. We note that one of the three related individuals previously reported by Tsai et al. (2002) with a diagnosis of THS was described to have coloboma of the iris and retina; however, exome analysis 15 years later revealed a known pathogenic variant in *ACTG1* [c.209C > T p.(Pro70Leu)], leading to a revised diagnosis of Baraitser–Winter syndrome (BWS) (Tsai et al. 2018). This is consistent with our previous observation that subjects in this family resembled individuals with BWS (Bhoj et al. 2019). Given the different molecular etiology, we excluded these individuals for further discussion in the context of THS.

We reviewed the 16 other individuals who were well-documented in the literature with THS but without a molecular diagnosis (Teebi 1987; Koenig 2003; Machado-Paula and Guion-Almeida 2003; Nakagawa et al. 1998; Stratton 1991; Toriello and Delp 1994; Tsukahara et al. 1995; Han et al. 2006) and found phenotypic features overlap considerably with the subjects summarized here. These features include recognizable craniofacial dysmorphism including hypertelorism, proptosis, ptosis, a broad forehead, broad and thick eyebrows, a short nose with a broad and/or depressed nasal root, and a thin upper lip; minor abnormalities of extremities such as clinodactyly, mild syndactyly, and small hands and feet; congenital heart defects; and umbilical defects (Table 1). Similarly, substantial craniofacial overlap was also noted between *SPECC1L*-associated hypertelorism syndrome (Bhoj et al. 2015, 2019; Zhang et al. 2020; Kruszka et al. 2015) and this cohort (Table 1). Interestingly,

among these shared craniofacial features, the occurrence of a depressed nasal root seems to be largely different between the two groups. Specifically, individuals with *SPECC1L*-associated hypertelorism syndrome generally have a broad nasal root and tend to have a high nasal root (100%) whereas 8 individuals (Teebi 1987; Nakagawa et al. 1998; Tsukahara et al. 1995) with THS in the literature (62%) and 13 individuals from our cohort (68%) have a depressed nasal root. This may help clinically distinguish *CDH11*-related THS from *SPECC1L*-related hypertelorism syndrome. The broad nasal root in individual 4 is probably related to her ethnic background. As previously speculated by us (Bhoj et al. 2019), it is suggested that these eight individuals with a clinical diagnosis of THS without a molecular diagnosis should be considered for *SPECC1L* gene sequencing, and now including *CDH11* as well. Furthermore, craniosynostosis and diaphragmatic hernia were absent in our cohort, while they were occasionally observed in *SPECC1L*-associated hypertelorism syndrome (19–23%) (Bhoj et al. 2019).

The converging phenotypes of patients with variants in *SPECC1L* or *CDH11* genes highlight the relevance of balanced cadherin expression during craniofacial morphogenesis. Indeed, the correct delamination of cranial neural crest (CNC) cells from the neuroectodermal epithelium, their migration toward the head and branchial arches and differentiation in several different tissues rely on an epithelial-to-mesenchymal transition (EMT) process, characterized by downregulation of type I cadherins (i.e., CDH1 and CDH2) and increased expression of the type II cadherin CDH11 (Kimura et al. 1995; Alimperti and Andreadis 2015). Of note, SPECC1L has recently been identified as a novel regulator of adherens junction stability through PI3K-AKT, and loss of SPECC1L expression in mouse embryos results in increased CDH1 levels, augmented adherens junction stability and defects in cranial neural crest cell delamination (Wilson et al. 2016). Similarly, CDH1 overexpression in the neural folds shows reduced or delayed delamination of the CNC cells (Taneyhill 2008; Theveneau and Mayor 2012). Conversely, reduction of CDH11 adhesive function results in non-directional and incomplete CNC cell migration in Xenopus models (Becker et al. 2013).

It has been recognized in the cancer field that upregulation of CDH11, resulting in changes in cellular function including cell migration, invasion, and epithelial-to-mesenchymal transition, correlated with tumor progression (Huang et al. 2010; Marchong et al. 2010; Li et al. 2012; Tomita et al. 2000; Pishvaian et al. 1999). Analyzing all of *CDH11* variants reported in cancer subjects from cBioPortal database (Gao et al. 2013) (n = 83,238 subjects and queried on April 7th, 2020) returned 1084 unique somatic variants. Among these, c.778G > A p.(Asp260Asn) was found in three subjects, with one having bladder urothelial carcinoma and two having uterine endometrioid carcinoma. However, to date there is no suggestion of an increased susceptibility to malignancy in association with germline *CDH11* variants.

Recently, a variety of genes have been implicated in several allelic syndromes with both autosomal recessive and dominant modes of inheritance (Esmaeeli Nieh et al. 2015; Motta et al. 2019; Meyer-Schuman and Antonellis 2017; Nabais Sa et al. 2019), such as *KIF1A*, *LZTR1*, *DEAF1*, *AARS*, *YARS*, *GARA*, and *HARS*. Homozygous (or compound heterozygous) loss-of-function (LoF) variants, including nonsense, frameshift, splice-altering, and missense, in *KIF1A* leading to motor and sensory neuron degeneration

in in vitro studies have been implicated in hereditary sensory and autonomic neuropathy and hereditary spastic paraplegia phenotype, whereas de novo dominant variants of *KIF1A* in the kinesin motor domain affecting the kinesin-mediated cargo transport in a dominant negative manner result in progressive encephalopathy and brain atrophy (Esmaeeli Nieh et al. 2015). Similarly, a number of genes (i.e., *AARS*, *YARS*, *GARA*, and *HARS*) encoding aminoacyl-tRNA synthetases can cause both dominant and recessive disorders through dominant negative and LoF effects, respectively (Meyer-Schuman and Antonellis 2017). Another well-known example would be Noonan syndrome due to either dominant negative or recessive LoF variants in *LZTR1* (Motta et al. 2019). Most recently, both dominant negative and recessive LoF variants in a previously known gene for autism, *DEAF1*, also identified to cause a spectrum of neurodevelopmental disorders (Nabais Sa et al. 2019). Our study further supports the concept of allelic syndromes with different inheritance patterns due to different variants' biological functions.

Conclusion

We report 19 individuals from 9 families with a clinical diagnosis of THS and heterozygous missense variants in *CDH11*. Following the recent recommendation to name Mendelian genetic disorders (Biesecker et al. 2021), we propose *CDH11*-related THS for this cohort of patients. In vitro functional assessment demonstrated that all of the six studied variants affect the cell–cell *trans* adhesion function or accelerated cell migration, supporting a disease mechanism. Compared to individuals with *SPECC1L*-related hypertelorism syndrome with a high prevalence of broad/high nasal root, subjects with *CDH11*-related THS tend to have a depressed nasal root. In general, *CDH11*-related THS is associated with a more variable, less severe phenotype with less pronounced dysmorphic features and generally normal or only mildly delayed development compared to *CDH11*-related EWS. There are also differences in associated structural features, with cardiac or umbilical defects being features of *CDH11*-related THS and skeletal anomalies in *CDH11*-related EWS. Advances in our understanding of the emerging spectrum of THS and phenotype associated with heterozygous *CDH11* variant will benefit families by facilitating counselling and aiding in reproductive decision making.

Supplementary Material

Refer to Web version on PubMed Central for supplementary material.

Acknowledgements

We thank all the families involved in this study for their participation.

Funding

Research reported in this publication was supported in part by the Roberts Collaborative Functional Genomics Rapid Grant (to D.L., C.S., L.P.) from CHOP. The research conducted at the Murdoch Children's Research Institute was supported by the Victorian Government's Operational Infrastructure Support Program. F.B. acknowledges for support and is member of the Italian Undiagnosed Rare Diseases Network led by Dr. Domenica Taruscio (Director, National Centre for Rare Diseases, Istituto Superiore Sanità, Italy). We would like to thank Prof. Ian Glass and Mei Deng, Birth Defects Research Laboratory, University of Washington, for conceptual tissues.

Data availability

The variants are available in the Leiden Open Variation Database (LOVD, www.LOVD.nl/CDH11).

References

Accogli A, Calabretta S, St-Onge J, Boudrahem-Addour N, Dionne-Laporte A, Joset P, Azzarello-Burri S, Rauch A, Krier J, Fieg E et al. (2019) De novo pathogenic variants in N-cadherin cause a syndromic neurodevelopmental disorder with corpus callosum, axon, cardiac, ocular, and genital defects. Am J Hum Genet 105:854–868 [PubMed: 31585109]

Alimperti S, Andreadis ST (2015) CDH2 and CDH11 act as regulators of stem cell fate decisions. Stem Cell Res 14:270–282 [PubMed: 25771201]

Becker SF, Mayor R, Kashef J (2013) Cadherin-11 mediates contact inhibition of locomotion during Xenopus neural crest cell migration. PLoS ONE 8:e85717 [PubMed: 24392028]

Bhoj EJ, Li D, Harr MH, Tian L, Wang T, Zhao Y, Qiu H, Kim C, Hoffman JD, Hakonarson H et al. (2015) Expanding the SPECC1L mutation phenotypic spectrum to include Teebi hypertelorism syndrome. Am J Med Genet A 167A:2497–2502 [PubMed: 26111080]

Bhoj EJ, Haye D, Toutain A, Bonneau D, Nielsen IK, Lund IB, Bogaard P, Leenskjold S, Karaer K, Wild KT et al. (2019) Phenotypic spectrum associated with SPECC1L pathogenic variants: new families and critical review of the nosology of Teebi, Opitz GBBB, and Baraitser–Winter syndromes. Eur J Med Genet 62:103588 [PubMed: 30472488]

Biesecker LG, Adam MP, Alkuraya FS, Amemiya AR, Bamshad MJ, Beck AE, Bennett JT, Bird LM, Carey JC, Chung B et al. (2021) A dyadic approach to the delineation of diagnostic entities in clinical genomics. Am J Hum Genet 108:8–15 [PubMed: 33417889]

Borchers A, David R, Wedlich D (2001) Xenopus cadherin-11 restrains cranial neural crest migration and influences neural crest specification. Development 128:3049–3060 [PubMed: 11688555]

Brasch J, Harrison OJ, Honig B, Shapiro L (2012) Thinking outside the cell: how cadherins drive adhesion. Trends Cell Biol 22:299–310 [PubMed: 22555008]

Brito LA, Yamamoto GL, Melo S, Malcher C, Ferreira SG, Figueiredo J, Alvizi L, Kobayashi GS, Naslavsky MS, Alonso N et al. (2015) Rare variants in the epithelial cadherin gene underlying the genetic etiology of nonsyndromic cleft lip with or without cleft palate. Hum Mutat 36:1029–1033 [PubMed: 26123647]

Castori M, Ott CE, Bisceglia L, Leone MP, Mazza T, Castellana S, Tomassi J, Lanciotti S, Mundlos S, Hennekam RC et al. (2018) A novel mutation in CDH11, encoding cadherin-11, cause branchioskeletogenital (Elsahy–Waters) syndrome. Am J Med Genet A 176:2028–2033 [PubMed: 30194892]

Cavey M, Rauzi M, Lenne PF, Lecuit T (2008) A two-tiered mechanism for stabilization and immobilization of E-cadherin. Nature 453:751–756 [PubMed: 18480755]

Chappuis-Flament S, Wong E, Hicks LD, Kay CM, Gumbiner BM (2001) Multiple cadherin extracellular repeats mediate homophilic binding and adhesion. J Cell Biol 154:231–243 [PubMed: 11449003]

Corso G, Roviello F, Paredes J, Pedrazzani C, Novais M, Correia J, Marrelli D, Cirnes L, Seruca R, Oliveira C et al. (2007) Characterization of the P373L E-cadherin germline missense mutation and implication for clinical management. Eur J Surg Oncol 33:1061–1067 [PubMed: 17434710]

Cox LL, Cox TC, Moreno Uribe LM, Zhu Y, Richter CT, Nidey N, Standley JM, Deng M, Blue E, Chong JX et al. (2018) Mutations in the epithelial cadherin-p120-catenin complex cause Mendelian non-syndromic cleft lip with or without cleft palate. Am J Hum Genet 102:1143–1157 [PubMed: 29805042]

Esmaeeli Nieh S, Madou MR, Sirajuddin M, Fregeau B, McKnight D, Lexa K, Strober J, Spaeth C, Hallinan BE, Smaoui N et al. (2015) De novo mutations in KIF1A cause progressive encephalopathy and brain atrophy. Ann Clin Transl Neurol 2:623–635 [PubMed: 26125038]

Gao J, Aksoy BA, Dogrusoz U, Dresdner G, Gross B, Sumer SO, Sun Y, Jacobsen A, Sinha R, Larsson E et al. (2013) Integrative analysis of complex cancer genomics and clinical profiles using the cBioPortal. Sci Signal 6:l1

Ghoumid J, Stichelbout M, Jourdain AS, Frenois F, Lejeune-Dumoulin S, Alex-Cordier MP, Lebrun M, Guerreschi P, Duquennoy-Martinot V, Vinchon M et al. (2017) Blepharocheilodontic syndrome is a CDH1 pathway-related disorder due to mutations in CDH1 and CTNND1. Genet Med 19:1013–1021 [PubMed: 28301459]

Guex N, Peitsch MC (1997) SWISS-MODEL and the Swiss-Pdb-Viewer: an environment for comparative protein modeling. Electrophoresis 18:2714–2723 [PubMed: 9504803]

Guilford P, Hopkins J, Harraway J, McLeod M, McLeod N, Harawira P, Taite H, Scoular R, Miller A, Reeve AE (1998) E-cadherin germline mutations in familial gastric cancer. Nature 392:402–405 [PubMed: 9537325]

Han XD, Cox V, Slavotinek A (2006) Atrioventricular block and wiry hair in Teebi hypertelorism syndrome. Am J Med Genet A 140:1960–1964 [PubMed: 16906548]

Harms FL, Nampoothiri S, Anazi S, Yesodharan D, Alawi M, Kutsche K, Alkuraya FS (2018) Elsahy–Waters syndrome is caused by biallelic mutations in CDH11. Am J Med Genet A 176:477–482 [PubMed: 29271567]

Hoffman JD, Irons M, Schwartz CE, Medne L, Zackai EH (2007) A newly recognized craniosynostosis syndrome with features of Aarskog–Scott and Teebi syndromes. Am J Med Genet A 143A:1282–1286 [PubMed: 17506099]

Huang CF, Lira C, Chu K, Bilen MA, Lee YC, Ye X, Kim SM, Ortiz A, Wu FL, Logothetis CJ et al. (2010) Cadherin-11 increases migration and invasion of prostate cancer cells and enhances their interaction with osteoblasts. Cancer Res 70:4580–4589 [PubMed: 20484040]

Hyafil F, Babinet C, Jacob F (1981) Cell–cell interactions in early embryogenesis: a molecular approach to the role of calcium. Cell 26:447–454 [PubMed: 6976838]

Kashef J, Kohler A, Kuriyama S, Alfandari D, Mayor R, Wedlich D (2009) Cadherin-11 regulates protrusive activity in Xenopus cranial neural crest cells upstream of Trio and the small GTPases. Genes Dev 23:1393–1398 [PubMed: 19528317]

Kawaguchi J, Takeshita S, Kashima T, Imai T, Machinami R, Kudo A (1999) Expression and function of the splice variant of the human cadherin-11 gene in subordination to intact cadherin-11. J Bone Miner Res 14:764–775 [PubMed: 10320525]

Kievit A, Tessadori F, Douben H, Jordens I, Maurice M, Hoogeboom J, Hennekam R, Nampoothiri S, Kayserili H, Castori M et al. (2018) Variants in members of the cadherin–catenin complex, CDH1 and CTNND1, cause blepharocheilodontic syndrome. Eur J Hum Genet 26:210–219 [PubMed: 29348693]

Kimura Y, Matsunami H, Inoue T, Shimamura K, Uchida N, Ueno T, Miyazaki T, Takeichi M (1995) Cadherin-11 expressed in association with mesenchymal morphogenesis in the head, somite, and limb bud of early mouse embryos. Dev Biol 169:347–358 [PubMed: 7750650]

Kitagawa M, Natori M, Murase S, Hirano S, Taketani S, Suzuki ST (2000) Mutation analysis of cadherin-4 reveals amino acid residues of EC1 important for the structure and function. Biochem Biophys Res Commun 271:358–363 [PubMed: 10799302]

Kjaer KW, Hansen L, Schwabe GC, Marques-de-Faria AP, Eiberg H, Mundlos S, Tommerup N, Rosenberg T (2005) Distinct CDH3 mutations cause ectodermal dysplasia, ectrodactyly, macular dystrophy (EEM syndrome). J Med Genet 42:292–298 [PubMed: 15805154]

Koenig R (2003) Teebi hypertelorism syndrome. Clin Dysmorphol 12:187–189 [PubMed: 14564158]

Kruszka P, Li D, Harr MH, Wilson NR, Swarr D, McCormick EM, Chiavacci RM, Li M, Martinez AF, Hart RA et al. (2015) Mutations in SPECC1L, encoding sperm antigen with calponin homology and coiled-coil domains 1-like, are found in some cases of autosomal dominant Opitz G/BBB syndrome. J Med Genet 52:104–110 [PubMed: 25412741]

Langhe RP, Gudzenko T, Bachmann M, Becker SF, Gonnermann C, Winter C, Abbruzzese G, Alfandari D, Kratzer MC, Franz CM et al. (2016) Cadherin-11 localizes to focal adhesions and promotes cell-substrate adhesion. Nat Commun 7:10909 [PubMed: 26952325]

Li L, Ying J, Li H, Zhang Y, Shu X, Fan Y, Tan J, Cao Y, Tsao SW, Srivastava G et al. (2012) The human cadherin 11 is a pro-apoptotic tumor suppressor modulating cell stemness through Wnt/

beta-catenin signaling and silenced in common carcinomas. Oncogene 31:3901–3912 [PubMed: 22139084]

Machado-Paula LA, Guion-Almeida ML (2003) Teebi hypertelorism syndrome: additional cases. Am J Med Genet A 117A:181–183 [PubMed: 12567419]

Marchong MN, Yurkowski C, Ma C, Spencer C, Pajovic S, Gallie BL (2010) CDH11 acts as a tumor suppressor in a murine retinoblastoma model by facilitating tumor cell death. PLoS Genet 6:e1000923 [PubMed: 20421947]

Meyer-Schuman R, Antonellis A (2017) Emerging mechanisms of aminoacyl-tRNA synthetase mutations in recessive and dominant human disease. Hum Mol Genet 26:R114–R127 [PubMed: 28633377]

Motta M, Fidan M, Bellacchio E, Pantaleoni F, Schneider-Heieck K, Coppola S, Borck G, Salviati L, Zenker M, Cirstea IC et al. (2019) Dominant Noonan syndrome-causing LZTR1 mutations specifically affect the Kelch domain substrate-recognition surface and enhance RAS-MAPK signaling. Hum Mol Genet 28:1007–1022 [PubMed: 30481304]

Nabais Sa MJ, Jensik PJ, McGee SR, Parker MJ, Lahiri N, McNeil EP, Kroes HY, Hagerman RJ, Harrison RE, Montgomery T et al. (2019) De novo and biallelic DEAF1 variants cause a phenotypic spectrum. Genet Med 21:2059–2069 [PubMed: 30923367]

Nakagawa M, Kondo M, Matsui A (1998) Teebi hypertelorism syndrome with tetralogy of Fallot. Am J Med Genet 77:345–347 [PubMed: 9632162]

Nishimura T, Takeichi M (2009) Remodeling of the adherens junctions during morphogenesis. Curr Top Dev Biol 89:33–54 [PubMed: 19737641]

Okazaki M, Takeshita S, Kawai S, Kikuno R, Tsujimura A, Kudo A, Amann E (1994) Molecular cloning and characterization of OB-cadherin, a new member of cadherin family expressed in osteoblasts. J Biol Chem 269:12092–12098 [PubMed: 8163513]

Patel SD, Ciatto C, Chen CP, Bahna F, Rajebhosale M, Arkus N, Schieren I, Jessell TM, Honig B, Price SR et al. (2006) Type II cadherin ectodomain structures: implications for classical cadherin specificity. Cell 124:1255–1268 [PubMed: 16564015]

Pettersen EF, Goddard TD, Huang CC, Couch GS, Greenblatt DM, Meng EC, Ferrin TE (2004) UCSF Chimera–a visualization system for exploratory research and analysis. J Comput Chem 25:1605–1612 [PubMed: 15264254]

Pishvaian MJ, Feltes CM, Thompson P, Bussemakers MJ, Schalken JA, Byers SW (1999) Cadherin-11 is expressed in invasive breast cancer cell lines. Cancer Res 59:947–952 [PubMed: 10029089]

Richards FM, McKee SA, Rajpar MH, Cole TR, Evans DG, Jankowski JA, McKeown C, Sanders DS, Maher ER (1999) Germline E-cadherin gene (CDH1) mutations predispose to familial gastric cancer and colorectal cancer. Hum Mol Genet 8:607–610 [PubMed: 10072428]

Saadi I, Alkuraya FS, Gisselbrecht SS, Goessling W, Cavallesco R, Turbe-Doan A, Petrin AL, Harris J, Siddiqui U, Grix AW Jr et al. (2011) Deficiency of the cytoskeletal protein SPECC1L leads to oblique facial clefting. Am J Hum Genet 89:44–55 [PubMed: 21703590]

Sobreira N, Schiettecatte F, Valle D, Hamosh A (2015) Gene-Matcher: a matching tool for connecting investigators with an interest in the same gene. Hum Mutat 36:928–930 [PubMed: 26220891]

Sprecher E, Bergman R, Richard G, Lurie R, Shalev S, Petronius D, Shalata A, Anbinder Y, Leibu R, Perlman I et al. (2001) Hypotrichosis with juvenile macular dystrophy is caused by a mutation in CDH3, encoding P-cadherin. Nat Genet 29:134–136 [PubMed: 11544476]

Stratton RF (1991) Teebi hypertelorism syndrome (brachycephalofrontonasal dysplasia) in a U.S. family. Am J Med Genet 39:78–80 [PubMed: 1867268]

Takeichi M (1995) Morphogenetic roles of classic cadherins. Curr Opin Cell Biol 7:619–627 [PubMed: 8573335]

Tamura K, Shan WS, Hendrickson WA, Colman DR, Shapiro L (1998) Structure-function analysis of cell adhesion by neural (N-) cadherin. Neuron 20:1153–1163 [PubMed: 9655503]

Taneyhill LA (2008) To adhere or not to adhere: the role of Cadherins in neural crest development. Cell Adh Migr 2:223–230 [PubMed: 19262148]

Taskiran EZ, Karaosmanoglu B, Kosukcu C, Dogan OA, Taylan-Sekeroglu H, Simsek-Kiper PO, Utine EG, Boduroglu K, Alikasifoglu M (2017) Homozygous indel mutation in CDH11 as the probable cause of Elsahy–Waters syndrome. Am J Med Genet A 173:3143–3152 [PubMed: 28988429]

Teebi AS (1987) New autosomal dominant syndrome resembling craniofrontonasal dysplasia. Am J Med Genet 28:581–591 [PubMed: 3425628]

Tepass U (1999) Genetic analysis of cadherin function in animal morphogenesis. Curr Opin Cell Biol 11:540–548 [PubMed: 10508657]

Tepass U, Truong K, Godt D, Ikura M, Peifer M (2000) Cadherins in embryonic and neural morphogenesis. Nat Rev Mol Cell Biol 1:91–100 [PubMed: 11253370]

Theveneau E, Mayor R (2012) Cadherins in collective cell migration of mesenchymal cells. Curr Opin Cell Biol 24:677–684 [PubMed: 22944726]

Tomita K, van Bokhoven A, van Leenders GJ, Ruijter ET, Jansen CF, Bussemakers MJ, Schalken JA (2000) Cadherin switching in human prostate cancer progression. Cancer Res 60:3650–3654 [PubMed: 10910081]

Toriello HV, Delp K (1994) Teebi hypertelorism syndrome: report of a third family. Clin Dysmorphol 3:335–339 [PubMed: 7894738]

Tsai AC, Robertson JR, Teebi AS (2002) Teebi hypertelorism syndrome: report of a family with previously unrecognized findings. Am J Med Genet 113:302–306 [PubMed: 12439902]

Tsai C, Shi Y, Liu T, Spector E, Roberson J, Meeks N (2018) Loss of function mutation of ACTG1 causes Teebi hyperteorism syndrome in 39th annual David W Smith workshop on malformations and morphogenesis Banff, Alberta, Canada

Tsukahara M, Uchida M, Shinohara T (1995) Teebi hypertelorism syndrome: further observations. Am J Med Genet 59:59–61 [PubMed: 8849013]

Vunnam N, Pedigo S (2011) Calcium-induced strain in the monomer promotes dimerization in neural cadherin. Biochemistry 50:8437–8444 [PubMed: 21870846]

Wiel L, Baakman C, Gilissen D, Veltman JA, Vriend G, Gilissen C (2019) MetaDome: pathogenicity analysis of genetic variants through aggregation of homologous human protein domains. Hum Mutat 40:1030–1038 [PubMed: 31116477]

Wilson NR, Olm-Shipman AJ, Acevedo DS, Palaniyandi K, Hall EG, Kosa E, Stumpff KM, Smith GJ, Pitstick L, Liao EC et al. (2016) SPECC1L deficiency results in increased adherens junction stability and reduced cranial neural crest cell delamination. Sci Rep 6:17735 [PubMed: 26787558]

Yagi T, Takeichi M (2000) Cadherin superfamily genes: functions, genomic organization, and neurologic diversity. Genes Dev 14:1169–1180 [PubMed: 10817752]

Zhang T, Wu Q, Zhu L, Wu D, Yang R, Qi M, Huang X (2020) A novel SPECC1L mutation causing Teebi hypertelorism syndrome: expanding phenotypic and genetic spectrum. Eur J Med Genet 63:103851 [PubMed: 31953237]

Zhu B, Chappuis-Flament S, Wong E, Jensen IE, Gumbiner BM, Leckband D (2003) Functional analysis of the structural basis of homophilic cadherin adhesion. Biophys J 84:4033–4042 [PubMed: 12770907]

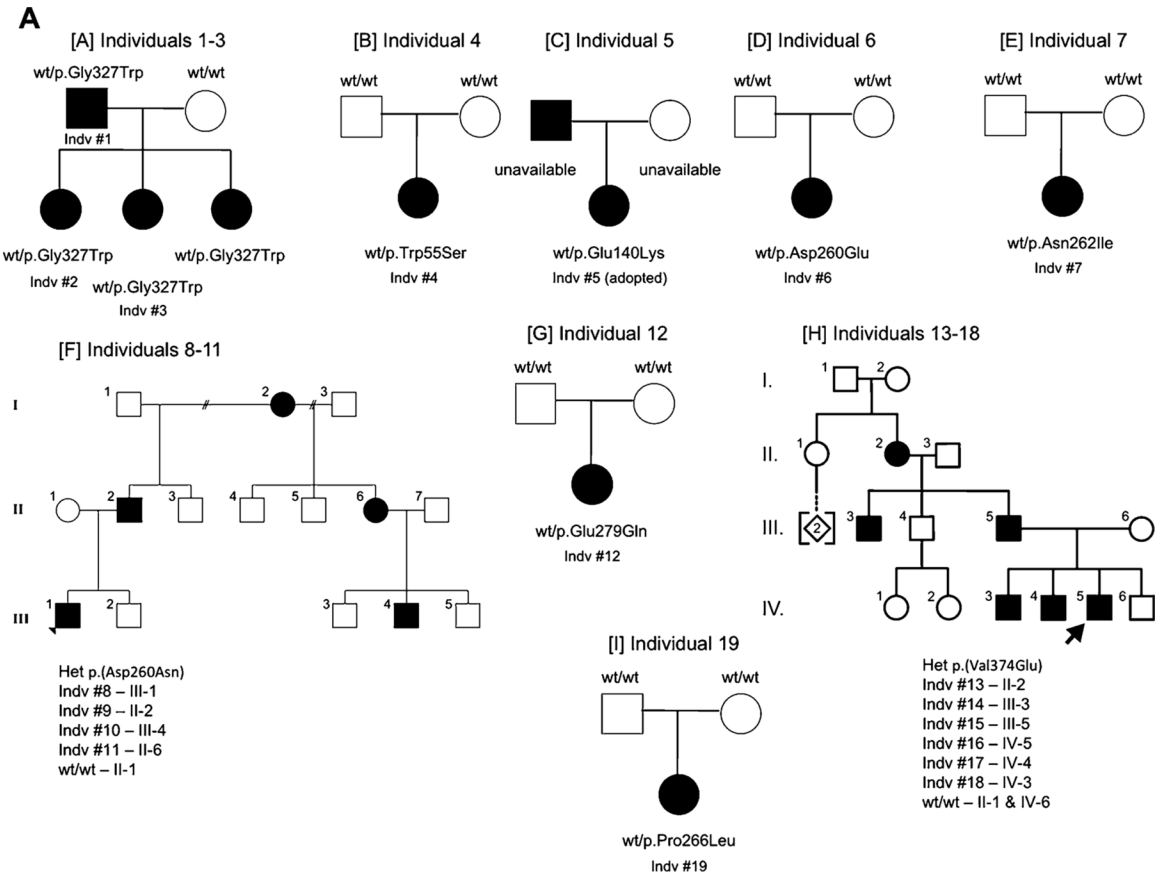

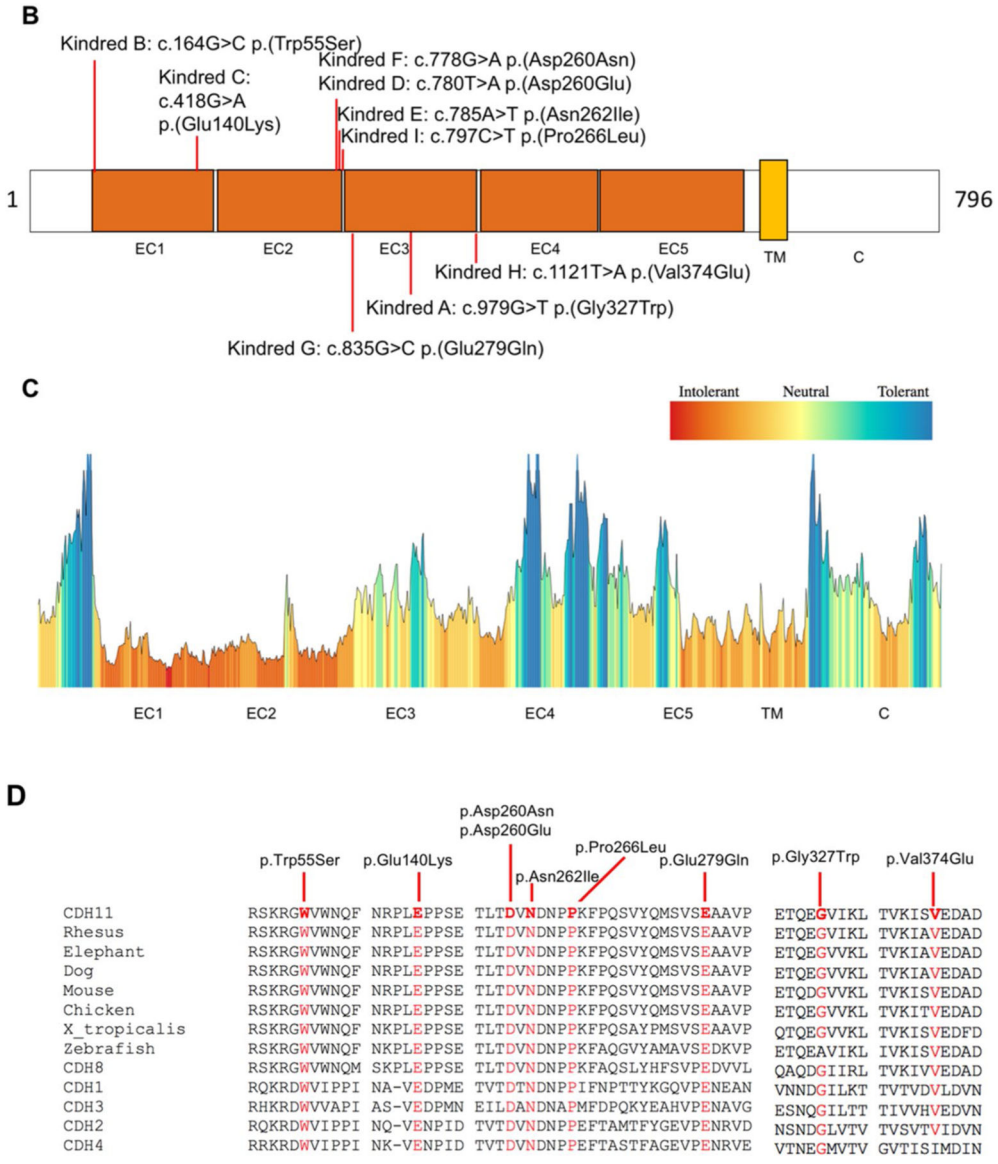

Fig. 1.

Molecular genetic findings in individuals with heterozygous *CDH11* variants. **a** Pedigrees and genotypes of de novo or dominantly inherited *CDH11* variants identified in nine kindreds A–I. **b** Schematic of CDH11 protein showing conserved domains and variants identified in kindreds A–I listed at the top and bottom. Conserved domains include five extracellular cadherin repeats (EC1–5), a transmembrane domain (TM), and a cytoplasmic tail (C). **c** An intolerance landscape plot generated by MetaDome for *CDH11* variant analysis. A ratio of d_N and d_S was calculated based on gnomAD population data and pathogenic variants from the ClinVar to profile genetic intolerance for protein domains. It showed EC1, EC2, and the EC1–EC2 and EC2–EC3 linker regions were the most intolerant EC repeats. **d** The affected residues highly conserved across vertebrate species and classical cadherins

Fig. 2.

Clinical images of individuals in this cohort include facial photographs, hands, and feet. Kindred and individual identifiers correlate with those in pedigrees and in Table S2

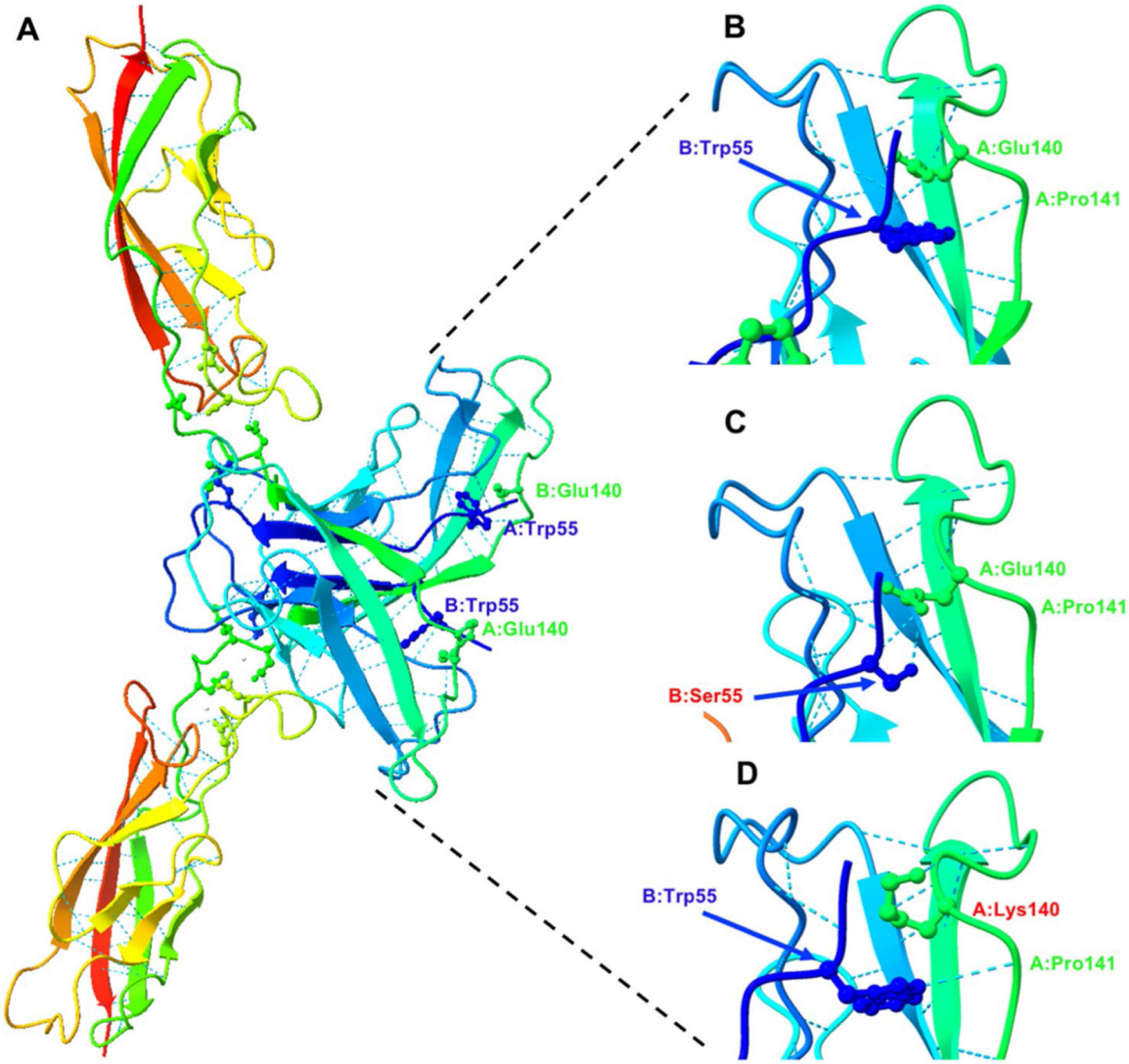

Fig. 3.

Three-dimensional structure analysis. **a** Three-dimensional structure modeling of CDH11 dimer using homology modeling with SWISS-MODEL (PDB: 2a4e). Residues Trp55 and Glu140 were shown with sticks. **b** Hydrophobic bonds between Trp55 and Glu140/ Pro141 from the partner chain. **c** Substitution of Trp55 with serine predicted to disrupt the hydrophobic bonds. **d** Replacement of Glu140 with lysine also predicted to disrupt the hydrophobic bonds with Trp55 from the partner chain

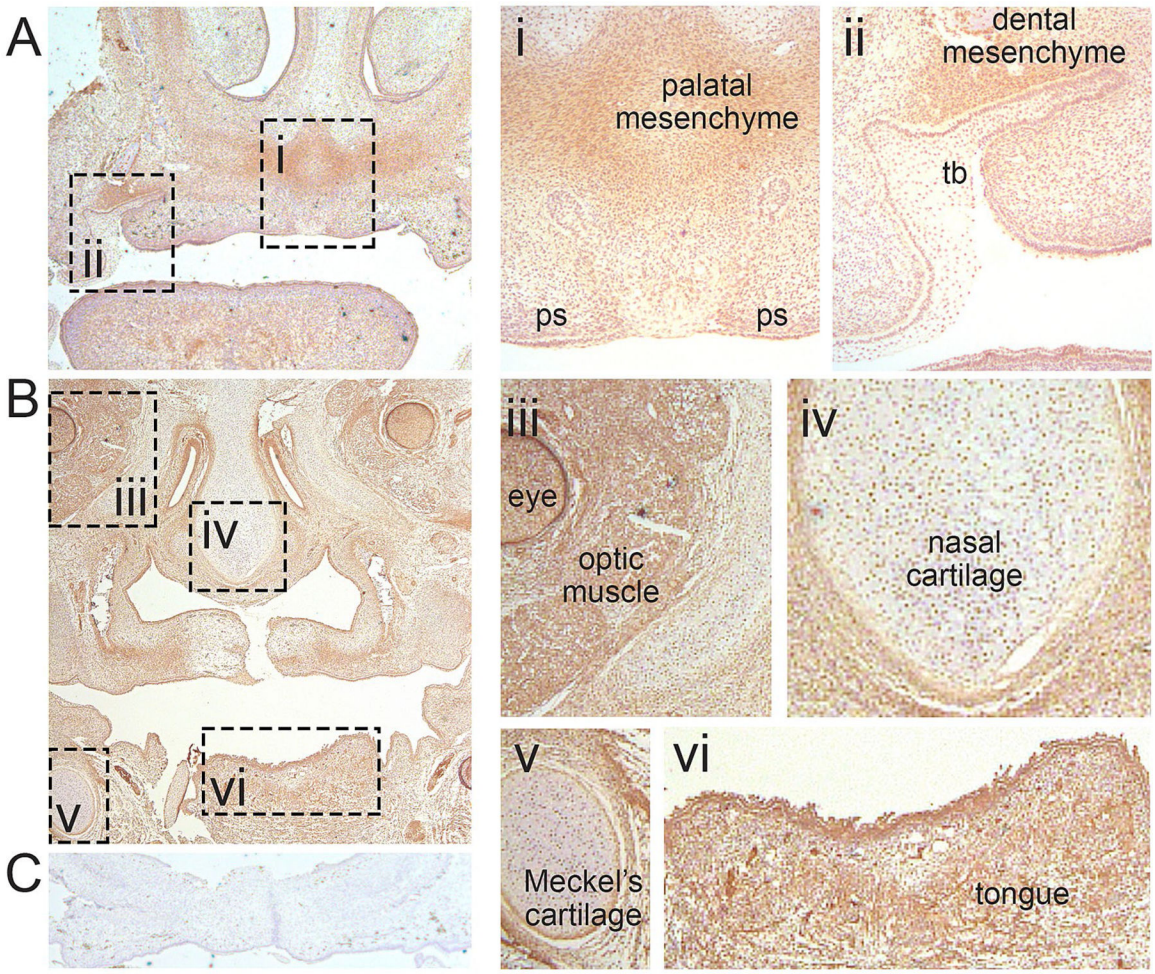

Fig. 4.

Immunohistochemical detection of CDH11 in coronal sections of 67–72d human embryonic facial tissue. Strong CDH11 staining is evident in facial mesenchyme at the mid-palatal region (**a**) as well as at the level of the posterior palate (**b**). **a** and **b** are sections from different facial specimens. Regions of strong staining include the central palatal mesenchyme (i), dental mesenchyme (ii), the eye and optic muscles (iii), and the tongue (vi). Both the nasal cartilage (iv) and Meckel's cartilage of the lower jaw (v) show negligible staining. **c** No primary antibody control

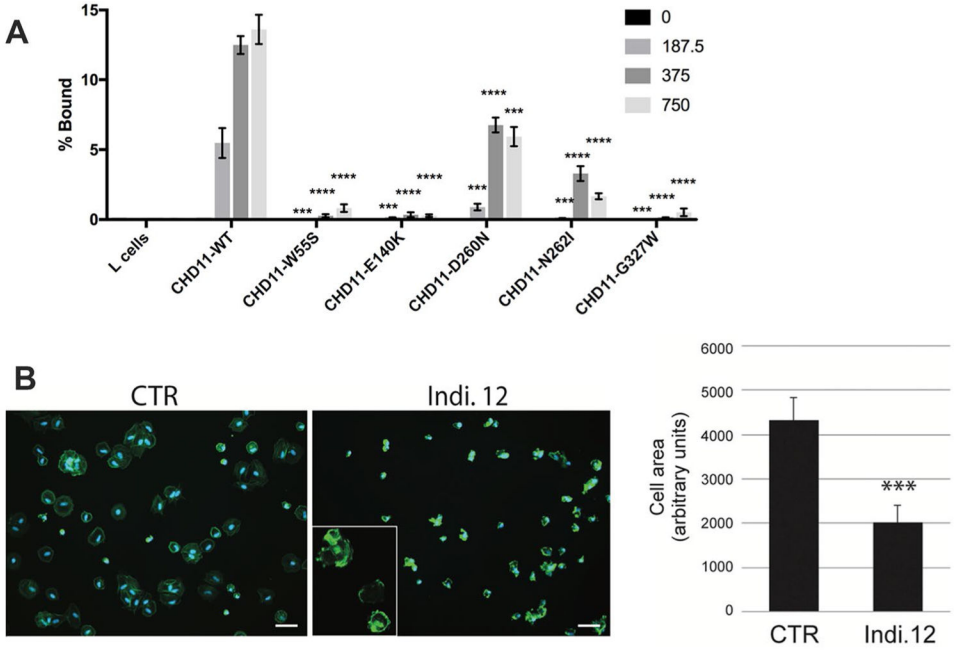

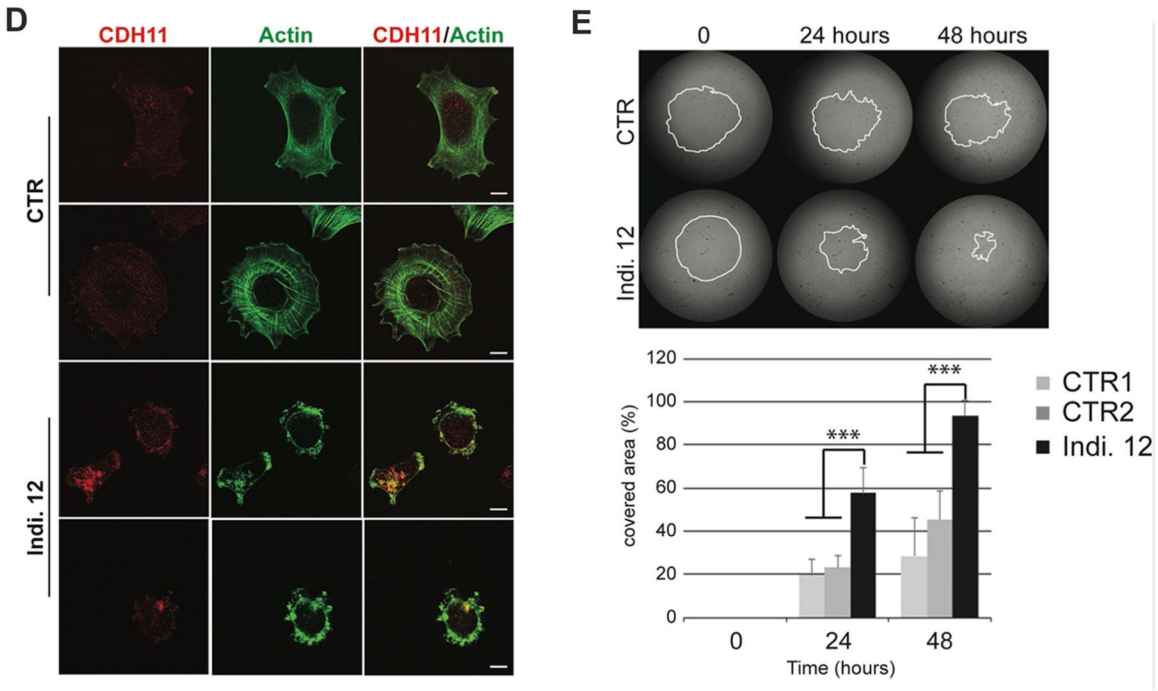

Fig. 5.

Heterozygous variants in *CDH11* change cell-substrate adhesion and migration property. **a** Cell-to-substrate adhesion assay showing L cells expressing five CDH11 mutants have consistently reduced *trans* adhesion at the hCadherin-11-Fc amount of 187.5, 375, and 750 ng. The data are shown as the mean ± s.e.m. of five independent experiments on an interleaved bar plot. Two-tailed paired *t* test, ***$P < 0.001$; ****$P < 0.0001$. **b** Actin staining (Actin-stain 488 Fluorescent Phalloidin, Cytoskeleton) of cells fixed 2 h after plating showing relevant morphological alteration of fibroblasts from individual 12 (Kindred G) with the p.(Glu279Gln) variant (Indi. 12) as compared to age-and sex-matched control cells (CTR). Insert, higher magnification showing peripheral blebs and ruffles and lack of stress fibers and lamellipodia in Indi. 12. Bar, 40 μm. The cell area was calculated using ImageJ software and plotted as mean area ± SD (on the right). Two different control cell strains were used. More than 600 cells from each population over three separate experiments were measured. ***$P < 0.005$. **c** Immunofluorescence analysis using anti-Paxillin monoclonal antibody (clone D9, Santa Cruz Biotechnology) and phalloidin showing abundance of immature focal adhesions not associated to actin stress fibers in individual 12 as compared to matched control cells. Bar, 20 μm. **d** Immunofluorescence analysis using anti-CDH11 monoclonal antibody (clone 5B2H5, ThermoFisher Scientific) and phalloidin showing protein aggregates colocalizing with actin bundles in fibroblasts from individual 12. Bar, 10 μm. **e** In vitro wound closure assays showing increased migration in fibroblasts from individual 12 as compared to control cells ($n = 2$). Representative images are shown from three independent time course cell migration experiments, each performed at least in triplicate. The white dotted lines define the areas lacking cells. The invaded area at 0, 24 and 48 h has been quantified using ImageJ software, and values of percentage of wound closure ± SD are shown in the graph below. ***$P < 0.005$

Table 1

Summary of clinical characteristics associated with heterozygous *CDH11* variant and comparison of the clinical features to three different cohorts

Clinical findings	**Individuals with *CDH11* het mutations in this study**	**Individuals in the literature carrying Teebi hypertelorism syndrome diagnosis***	**Individuals with *SPECC1L* missense variants#**	**Individuals with *CDH11* homozygous LoF variants**
Craniofacial				
Hypertelorism	19/19 (100%)	16/16 (100%)	31/32 (97%)	5/5 (100%)
Proptosis	5/19 (26%)	1/16 (6%)	None reported	5/5 (100%)
Ptosis	5/19 (26%)	10/16 (63%)	12/17 (71%)	None reported
Broad forehead	18/19 (95%)	11/16 (69%)	20/23 (87%)	5/5 (100%)
Broad, thick, or arched eyebrows	17/19 (89%)	16/16 (100%)	Frequent (> 80%)	5/5 (100%)
Eyelid coloboma	2/19 (11%)	None reported	None reported	1/5 (20%)
Short nose	15/19 (79%)	8/16 (50%)	Frequent; some have broad nose	5/5 (100%)
Broad or high nasal root	1/19 (5%)	13/16 (81%)	31/31 (100%)	5/5 (100%)
Depressed nasal root	13/19 (68%)	8/13 (62%)	0/31 (0%)	5/5 (100%)
Thin upper lip	16/19 (84%)	15/16 (94%)	Frequent	2/2 (100%)
Small chin with central transverse groove	16/19 (84%)	3/16 (19%)	12/21 (57%)	None reported
Developmental delay	7/19 (37%)	3/16 (19%)	12/19 (63%)	5/5 (100%)
Heart defect	5/19 (26%)	4/16 (25%)	7/24 (29%)	0/5 (0%)
Umbilical defect	3/13 (25%)	8/16 (50%)	11/22 (50%)	None reported
Truncal skeletal abnormality/vertebral fusion	3/13 (25%)	3/16 (19%)	Rare	2/3 (67%)
Hypospadias	4/8 (50%)	2/6 (33%)	0/14 (0%)	2/2 (100%)
Shawl scrotum	0/8 (0%)	2/6 (33%)	1/6 (17%)	None reported

*Exclude those individuals with SPECC1L mutations and three individuals, who were found to have *ACTG1* variant, reported by Tsai et al. (2002)

#Exclude the patient reported with oblique facial cleft reported by Saadi et al. (2011)